2

BNL-NUREG-26466
CONF-790760--2

VOID FLUCTUATION DYNAMICS AND MEASUREMENT TECHNIQUES

by

O.C. Jones, Jr., N. Abuaf, G.A. Zimmer, and T. Feierabend

Nuclear Safety Programs - Department of Nuclear Energy
Brookhaven National Laboratory, Upton, New York 11973

June 1979

MASTER

ABSTRACT

The current state of the art of void fluctuation dynamics and measurement techniques is briefly reviewed. New and improved measurement techniques which have been developed are described including two local probes which both have the capability of being responsive to phase presence and interfacial velocity. It is shown that the dynamics of a thin liquid film on optical probes have strong effects on the response not heretofore recognized.

Manuscript Prepared for Presentation at the Joint
U.S. - Japan Information Exchange on Two-Phase Flow Dynamics
Osaka University, Osaka, Japan
August 1-3, 1979

*Work performed under the auspices of the U.S. Nuclear Regulatory Commission

BNL-NUREG-26466

VOID FLUCTUATION DYNAMICS AND MEASUREMENT TECHNIQUES

by

O.C. Jones, Jr., N. Abuaf, G.A. Zimmer, and T. Feierabend

Nuclear Safety Programs - Department of Nuclear Energy
Brookhaven National Laboratory, Upton, New York 11973

June 1979

ABSTRACT

The current state of the art of void fluctuation dynamics and measurement techniques is briefly reviewed. New and improved measurement techniques which have been developed are described including two local probes which both have the capability of being responsive to phase presence and interfacial velocity. It is shown that the dynamics of a thin liquid film on optical probes have strong effects on the response not heretofore recognized.

Manuscript Prepared for Presentation at the Joint
U.S. - Japan Information Exchange on Two-Phase Flow Dynamics
Osaka University, Osaka, Japan
August 1-3, 1979

*Work performed under the auspices of the U.S. Nuclear Regulatory Commission

TABLE OF CONTENTS

LIST OF FIGURES

LIST OF FIGURES (Continued)

VOID FLUCTUATION DYNAMICS AND MEASUREMENT TECHNIQUES

1. INTRODUCTION

Void fluctuations are of interest in many areas such as related to thermal boundary layer renewal in heat transfer augmentation, bed stability in fluidized bed reactors or bubble contactors, recriticality due to density fluctuations in boiling fuel-steel mixtures in advanced reactor accident scenerios, pressure fluctuations as a source of instability in two-phase flow systems to name just a few. Applications appear in many current and advanced energy conversion and utilization systems that rely on the efficiencies of latent heat conversion for process dynamics. It seems fair to say that future gains in understanding the physics of two-phase dynamics, and in applying this understanding to improved design and optimization of energy systems will be based on grasping the fundamentals of liquid-vapor interactions through observation of their dynamic behavior. While the first useful considerations of fluctuation dynamics of liquid vapor systems were put forth more than a decade ago,[1-4] very little advance in understanding has been made since that time.

It appears reasonable that advances in understanding and predicting interphase transfer laws for mass, momentum, and energy will depend on observations of the phasic behavior coupled with the inference of these transfers from measured quantities. Observations of the phase fluctuation dynamics depends in turn on the development and utilization of appropriate measurement techniques. It is the purpose of this paper to review the status of our knowledge on void fluctuations and to discuss new methods developed for improved observation.

2. BACKGROUND

Void Fluctuation Dynamics

The only work which appears to have examined the macrostructure of two-phase, gas-liquid flows is reported in Reference 5. In this work, a fast response, linearized X-ray void measurement system has been used to obtain statistical measurements in normally fluctuating air-water flow in a rectangular channel. It is demonstrated that the probability density function (PDF) of the fluctuations in void fraction may be used as an objective and quantitative flow pattern discriminator for the three dominant patterns of bubbly, slug, and annular flow. This concept is applied to data over the range of 0.0 to 37m/sec mixture velocities to show that slug flow is simply a transitional, periodic time combination of bubbly and annular flows. Film thicknesses calculated from the PDF data are similar in magnitude in both slug and annular flows. Calculation of slug length and residence time ratios along with bubble lengths in slug flow are also readily obtainable from the statistical measurements. Spectral density measurements showed bubbly flow to be stochastic while slug and annular flows showed periodicites correlatable in terms of the liquid volume flux.

Typical of the results obtained are shown in Figures 1-4. In bubbly flows (Figure 1) the void fluctuations appear on the oscilloscope as small amplitude, randum fluctuations due to the stochositic appearance of small bubbles passing through the x-ray beam. The randomness is confirmed by the flat spectral density of the fluctuations. A probability density function representation of

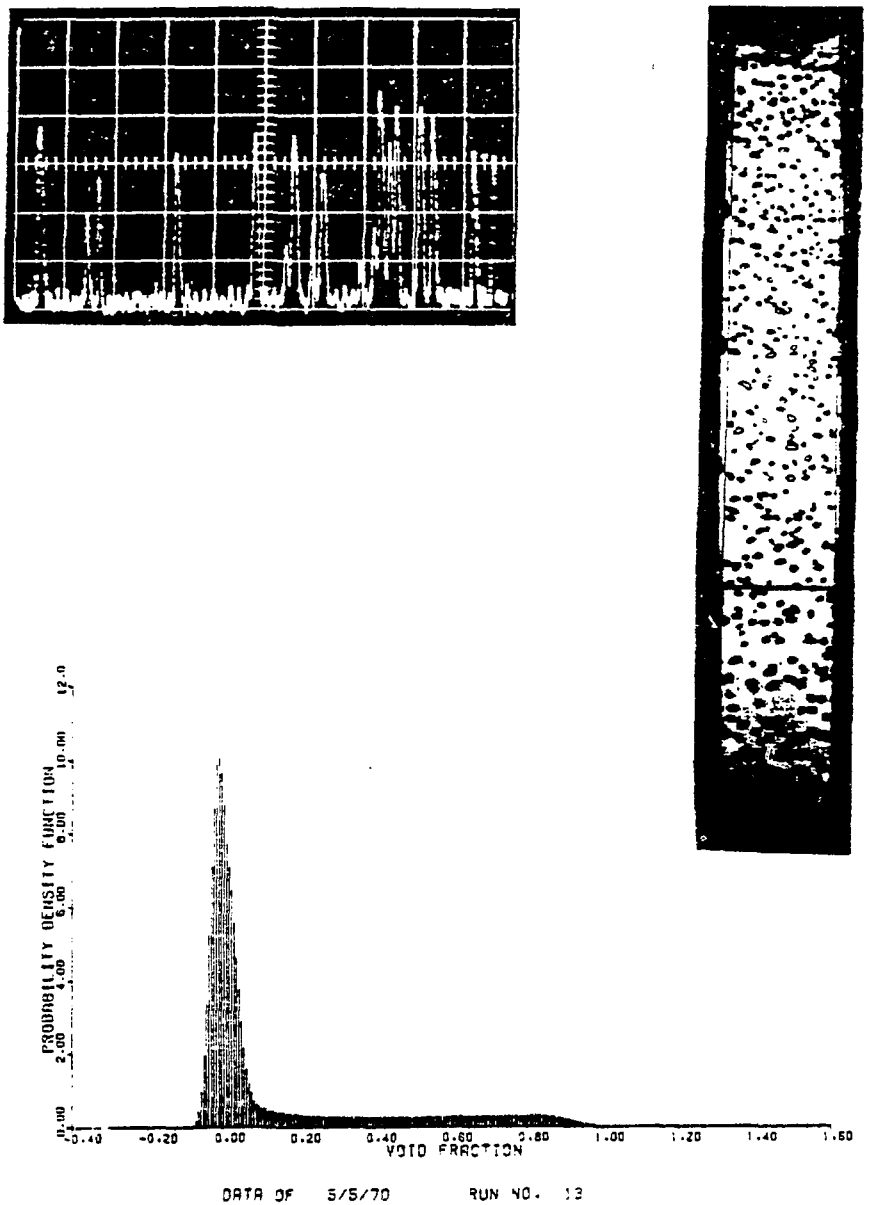

Figure 1 - Typical Determination of Statistical Void Fluctuation Behavior in Bubbly Flow

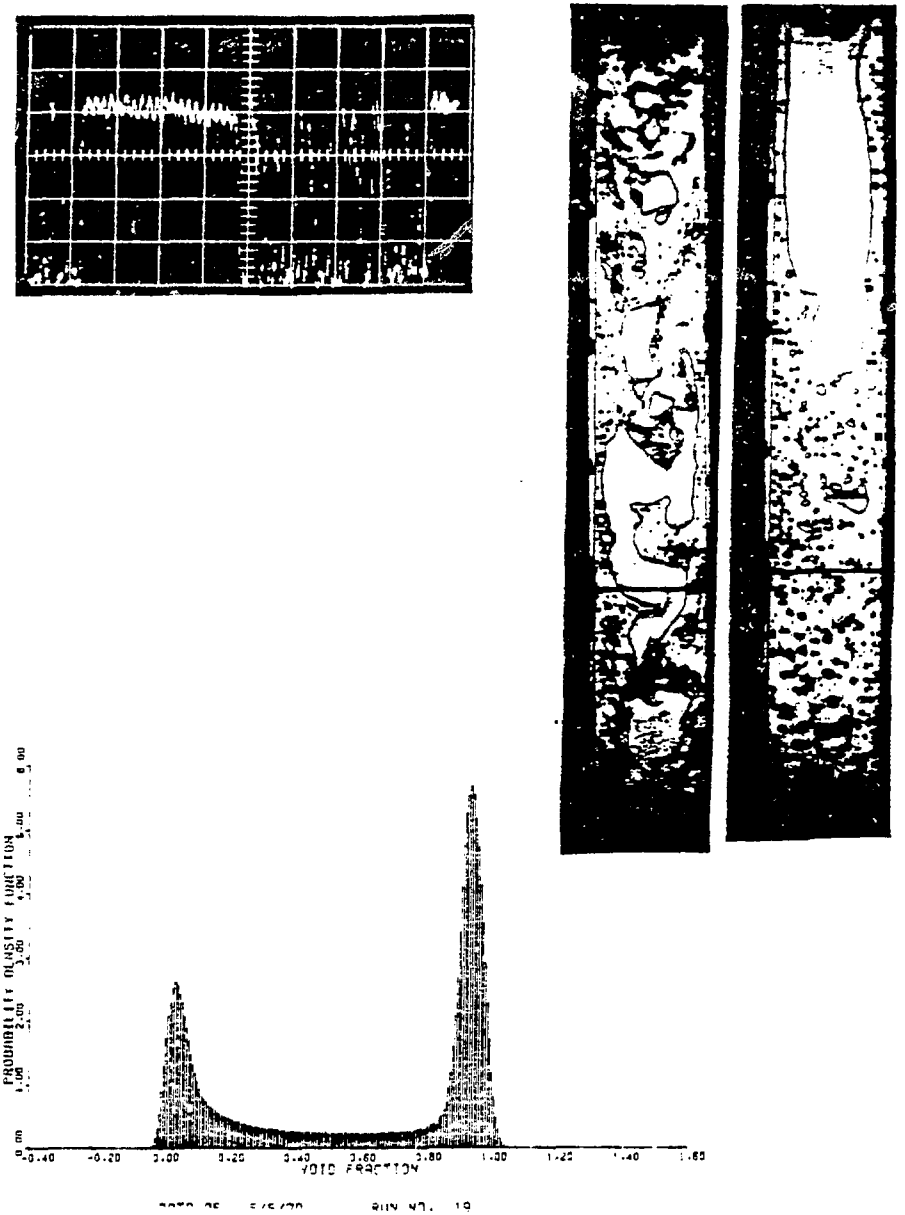

Figure 2 - Typical Determination of Statistical Void Fluctuation Behavior in Low Velocity Slug Flow

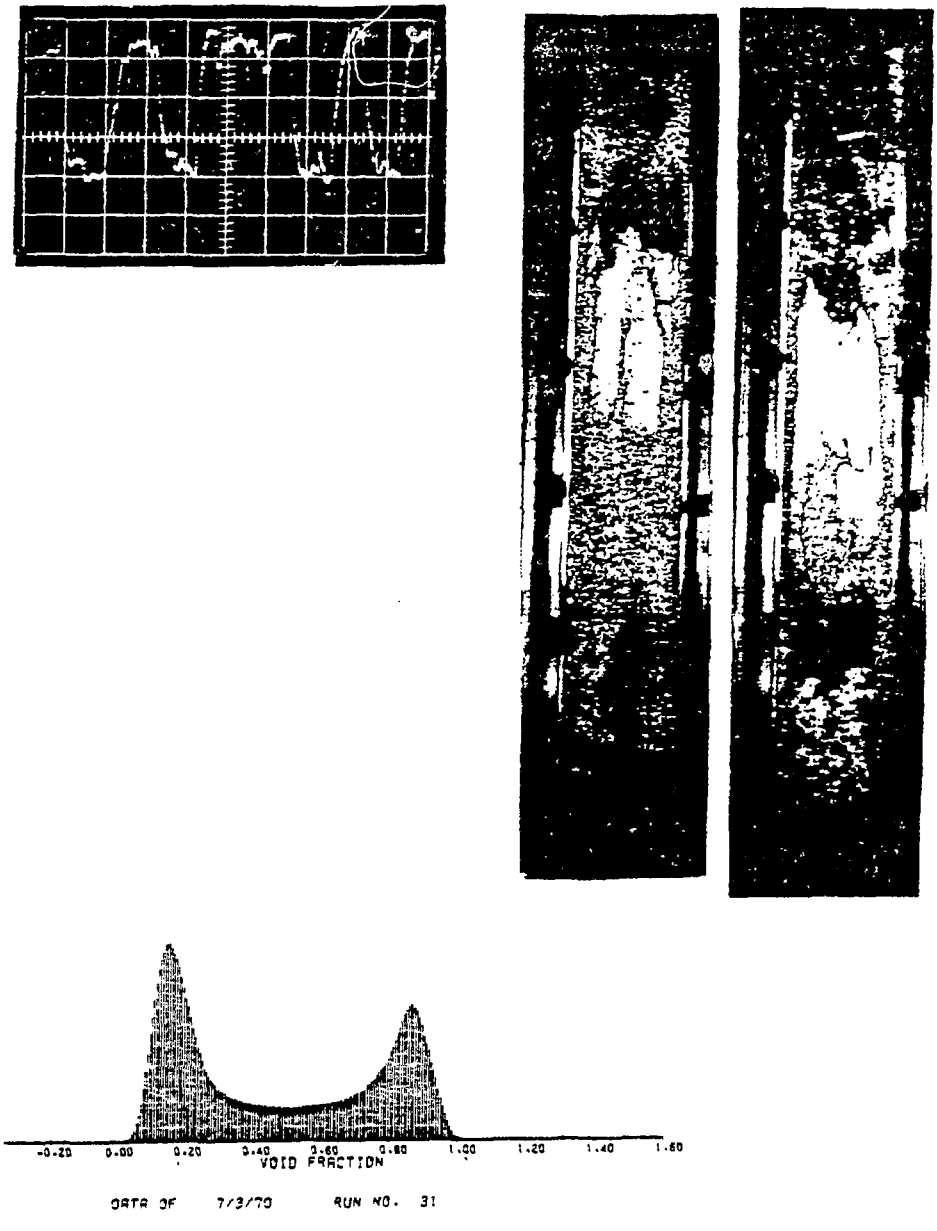

Figure 3 - Typical Determination of Statistical Void Fluctuation Behavior in High Velocity Slug Flow

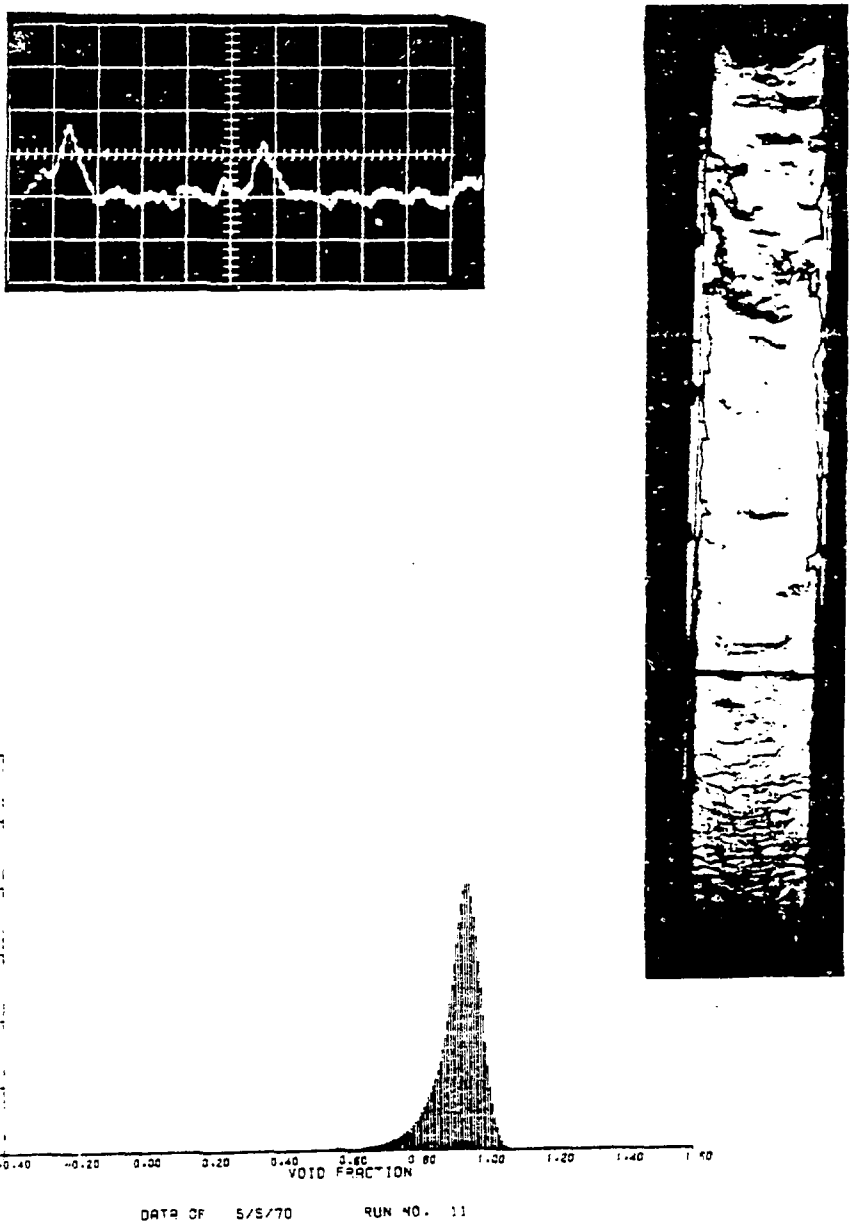

Figure 4 - Typical Determination of Statistical Void Fluctuation Behavior in Annular Flow

this case shows a single peak having a first moment equal to the mean void fraction and a standard deviation characteristic of the bubble size. Similar behavior is seen in annular flows (Figure 4) where the location of the mean occurs at a high void fraction characteristic of these flow patterns. In this case the standard deviation is a function of the waviness on the annular films and the size distributions of any droplet carried in roll waves or uniformly in the gaseous core.

Slug-like flows (including churn turbulent) from both a photographic viewpoint and from the oscillographic data appear as highly chaotic having significantly variable character (Figures 2 and 3). The PDF data, on the other hand, show a remarkably consistent pattern characteristic of a time combination of bubbly-and annular-like flows. This characterization is not very dissimilar from the ideas expressed by Ishagai, Yamone, and Roko[4].

While the spectra of the void fluctuations in bubbly flow were flat, typical of the stochastic nature of bubble passage, the void spectra for slug-like flows were strongly resonant at frequencies characteristic of the slug passage frequency, Figures 5 and 6.

In annular flows, the fluctuation spectra were mildly resonent indicative of smaller amplitude periodicities than observed in annular flows, Figures 7 and 8. It is noted that the dominant frequencies in annular flows are of similar order to those observed in slug-like flows. On the other hand, profiles of interfacial passage frequencies obtained by use of a hot film anemometer[6], Figure 9, are seen to be much larger than those of Figure 8, by 1-2 orders. The implication suggested from these comparisons is that the dominant frequencies in annular flow are due to low-density roll waves formed by the same or similar processes which form liquid slugs at lower void fractions in slug-like flows. The much higher frequencies associated with local interfacial passages are due to the small waviness on annular films, internal structure of roll waves, and droplet passages in the core.

Measurement Techniques

The obvious utility of X-rays as a measurement tool has been widely demonstrated and had lead to its broad utilization. In addition to obtaining mean chordal void fractions and the fluctuation data described in the previous section, other data are also obtainable including

a) film thicknesses in both annular flows and in the major bubbles in slug-like flows

b) slug residence time fractions

c) slug and bubble lengths.

One obvious advantage of X-rays over γ-rays, until recently, has been the ability of obtaining highly intense narrow beams of low energy, a very desirable characteristic for obtaining good sensitivity in metal-water systems, especially of small size. Power supplies, however, tend to be expensive and stabilization difficult so noise has been a continuing problem requiring diligent efforts to eliminate [5,7]. Low activation, low energy γ-ray sources have been used but high activations have been hampered due to low activation efficiencies, self shielding effects, and the like. Thus, γ-sources have generally relied on Co^{60} or Cs^{137}, especially for high pressure, thick walled systems. Alternate low energy sources such as Sa^{145}, Ga^{153}, or

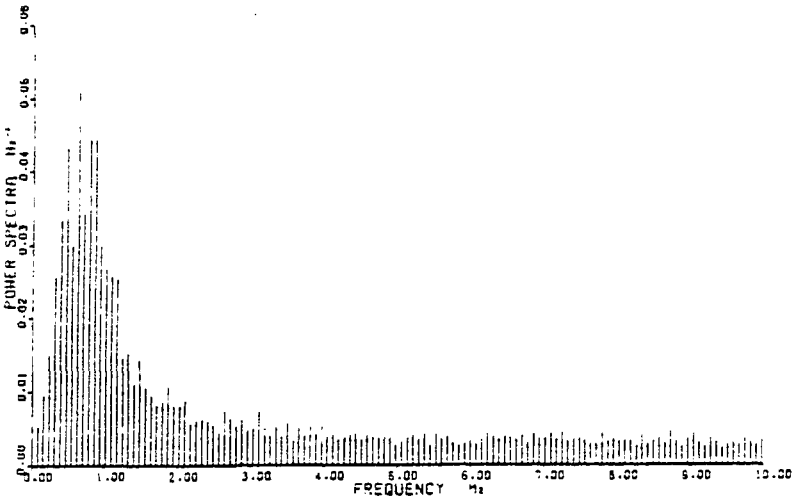

Figure 5 - Typical void fluctuation spectra for-slug-like flows.

Tm^{170} have had the disadvantage of generally low activation yielding poor time resolution due to nuclear statistics.

There have been several excellent summaries of two-phase measurement techniques [8-12], and no attempt to duplicate or summarize these works will be made herein. Other instruments utilized for transient and statistical diagnosis include:

a) Optical probes, the major difficulty has been signal processing (triggering) and apparent void dependency of the signal amplitude.

b) Microthermocouple - can't be used in adiabatic systems.

c) Hot film anemometry - fragility of the sensor, signal processing (triggering) remain difficult areas to overcome.

d) Electrical probes - signal processing (triggering), polarization, electrostatic charging present difficulties.

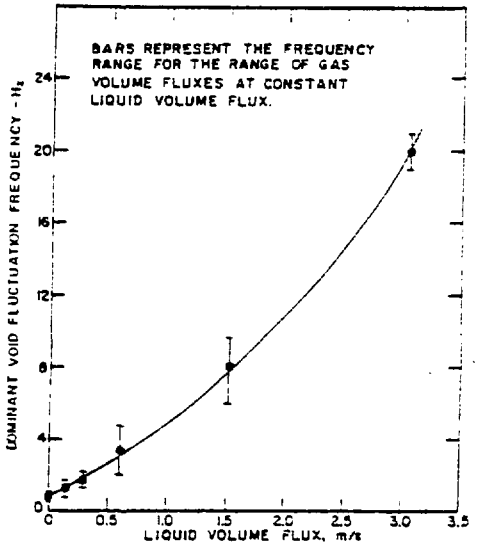

Figure 6 - Dominant void fluctuation frequencies in slug flow determined from the spectral density. (BNL Neg. No. 6-1320-79)

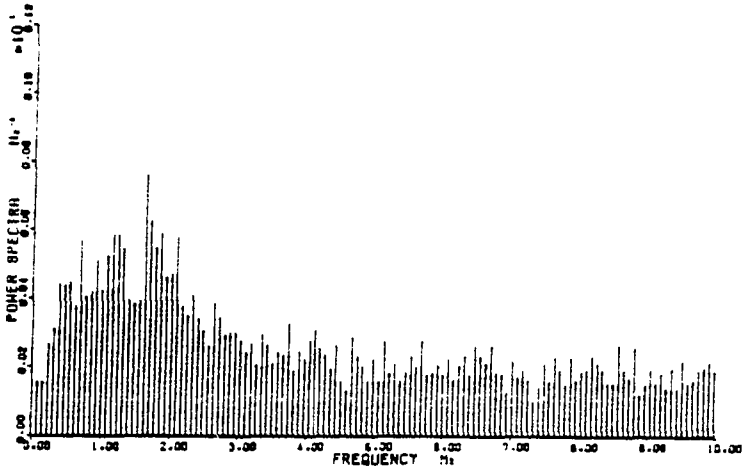

Figure 7 - Typical void fluctuation spectra for annular flows.

While single-sensor devices mentioned above have been used to obtain local measurements representative of void fraction all with similar accuracies estimated to be within 15%, dual-sensor probes have generally been required to provide information on velocities. With the exception of the hot film anemometer which has provided direct liquid velocity information, [13,14], all other instruments respond to phase presence so they track interfacial velocities by correlation techniques, rather than phase velocities. It has yet to be shown experimentally how average local interface velocity may be interpreted in terms of phase velocity. Recent reports from Prof. Ohba at Osaka University[15] indicate that laser-Doppler anemometry may prove more valuable in two phase flows than originally anticipated. Measurements of both liquid and gas velocities at void fractions up to 0.3 in bubbly mixtures have been reported.

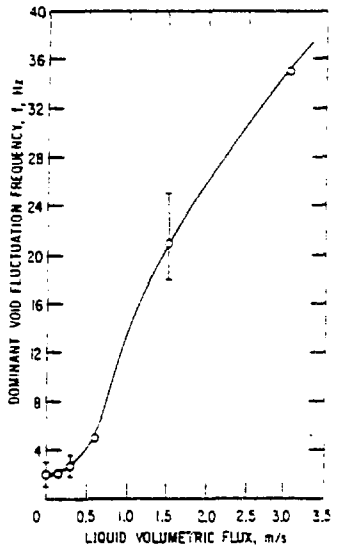

Figure 8 - Void fluctuation frequencies in annular flow. (BNL Neg. No. 6-1318-79)

While this brief summary seems to put void fluctuation dynamics and measurement techniques into perspective, recent advances have been made on several fronts. The balance of this paper shall be devoted to describing these advances.

3. IMPROVED MEASUREMENT TECHNIQUES

Gamma-Densitometer

An improved, high activation, low energy γ-densitometer system has been developed utilizing the 84 kev resonance of Tm^{170}. Activation of up to ~30 ci at 84 kev is being or shortly will be undertaken providing ~1.5% standard deviation in a system containing 5cm water and 1 mm of stainless steel in a 1.0 msec sample. Standard nuclear instrumentation coupled to a solid state cadmium teluride detector at room temperature provides the detection part of the system. This simplified new procedure is described in another session of this seminar and will not be duplicated here.[27]

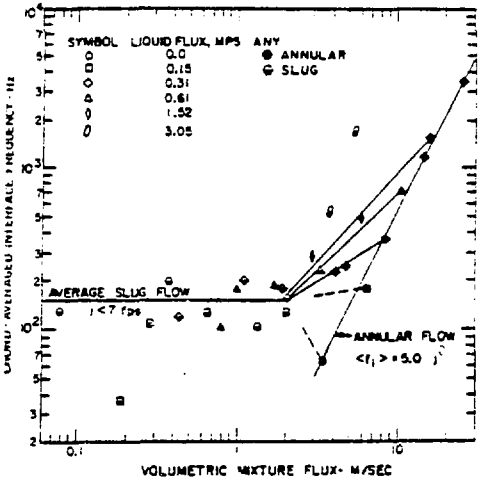

Figure 9 - Variations of chord-averaged interface passage frequencies with mixture volume flux in slug and annular flows. (BNL Neg. No. 6-1319-79)

Optical Probe

A new design optical probe was developed to circumvent the difficulties of variable signal levels previously reported.[16,17] The principal of operation is based on Snells law and has been previously described.[16,17,11]

A schematic of the probe as developed is depicted in Figure 10, with the light source and amplifier circuit diagram used in the apparatus. Two 125-um fibers were inserted into a 500-um-o.d. stainless-steel tube. The two fibers were fused together at one end by means of a minitorch, forming a spherical bead. This fused end of the fibers was then pulled into the tube and epoxied in place. The fibers were separated at the opposite end and encased in two pieces of stainless-steel tubing (250 μm o.d.). The ends of the fibers and the bifurcation were then epoxied for strength. The tip of the probe containing the fused end of the fibers was ground and polished at a 45° angle to the axes of the fibers, thus forming an included angle of 90° at the finished probe tip. After grinding and polishing the free ends of the two fibers flat, one of them was placed in front of an incandescent light source (3 V), and the other in front of a Hewlett-Packard PIN photodiode (5082-4024). An amplifier with a design rise time of 20 μs[12] was used to enhance the output before going into the readout device (Figure 10). The electronic response of the system was checked by means of a light-emitting diode (LED) placed in front of the probe tip. The LED output was modulated by using a signal generator so that light pulses of different spacings and widths were emitted, simulating the passage of bubbles. The rise time of the output was thus verified to be 20 μs as specified. The amplitude of the probe output did not change with the frequency of the input signal of the LED.

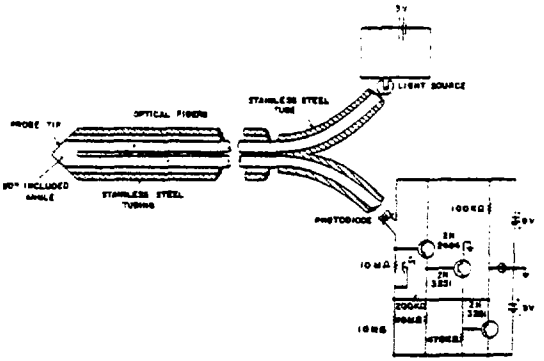

Figure 10 - Schematic representation of the optical probe.
(BNL Neg. No. 1-641-78)

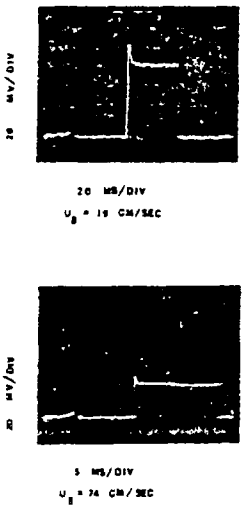

Figure 11 - Typical oscillograms of the output.
(BNL Neg. No. 9-111-77)

The hydrodynamic response of the probe to the passage of an interface or bubble was investigated as described in References 18 and 19, where single bubbles could be generated and forced past the probe while independent methods were used to determine the velocity. Typical oscillograms of the probe output during the passage of the bubble are presented in Figure 11. Here the probe output in mV is shown as a function of time for two cases where the bubble velocities were 19 and 74 cm/s, respectively. It was observed that when the tip was immersed in water the probe output was always zero without any artificial bias representing a significant change over previous optical probes. As the bubble hit the probe, the output was seen to increase, and after an overshoot, to level off to a certain steady value. At the end of the passage of the bubble the signal dropped to its original water level of zero. The bubble penetration time was clearly observed to be larger than the time it takes the probe tip to be immersed in water, Figure 12. Also the signal amplitude decreased with increasing bubble velocity, although both bubbles had almost the same length (void fraction), Figure 13. These two effects were investigated in some detail. Results obtained with two different probes are presented in Figure 13 as a function of bubble velocity. Although the two probes had a steady air signal amplitude of 125 and 600 mV, respectively, the ratio I/I_o follows the same consistent pattern.

A similar observation was noted by Miller and Mitchie, "With smaller bubbles and higher velocities. . . . The probe signal generated under these conditions. . . never reached maximum amplitude."[20]

An important conclusion that can be drawn from Figure 13 is that the optical probe is able to measure the local interface velocity as well as the local void fraction, after proper calibration within the velocity range observed.

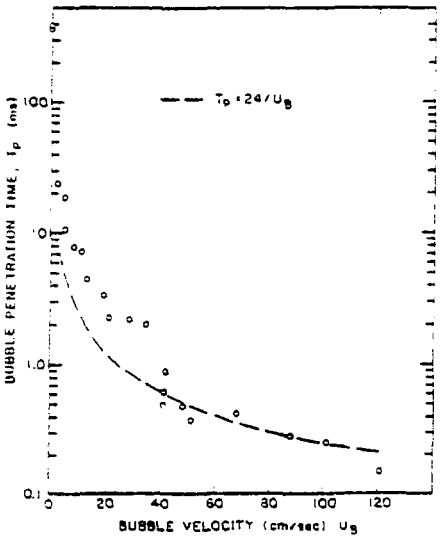

Figure 12 - Bubble penetration time vs. bubble velocity. (BNL Neg. No. 1-643-78)

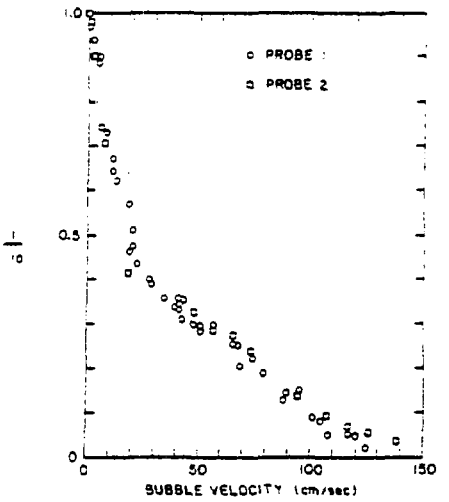

Figure 13 - Probe signal at a given bubble velocity, I, divided by the steady air signal, I_o, vs. bubble velocity. (BNL Neg. No. 1-650-78)

A computer program was written to study the theoretical response of the output to hydrodynamic conditions at the tip of the probe by tracing individual rays of light from their source to the detector. The effects of varying liquid film thicknesses on the the probe tip was included. Comparison of the geometric effects for the probe of Danel and Delhaye[16] and the new design are shown in Figure 14 where the new geometry is seen to be dependent on probe tip angle.

Computer calculations were also extended to study the signal attenuation that would be experienced when a variable film thickness is present at the probe tip. The water layer was assumed to increase linearly along the flat face. β is defined as the angle between the outside face of the water layer in contact with the air and the glass face of the probe tip in contact with the water layer. The attenuation of the rays during their passage from one media to another was not taken into account. Although the 104° total angle gave a higher signal in air when compared to the 90° total angle probe tip,

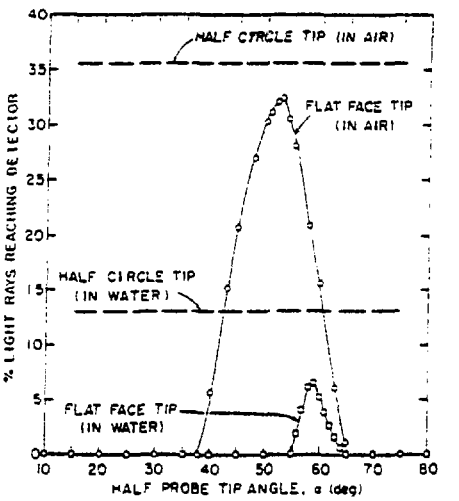

Figure 14 - Percent of light rays reaching the detector as a function of the half probe tip angle for the cases of the probe tip in air and in water. Comparison between the half circle and the flat face probe tips. (BNL Neg. No. 1-646-78)

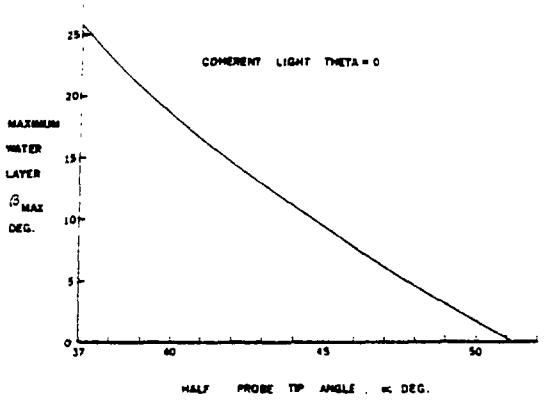

Figure 15 - Maximum thickness of water layer on the flat face probe tip for zero output.
(BNL Neg. No. 3-1722-78)

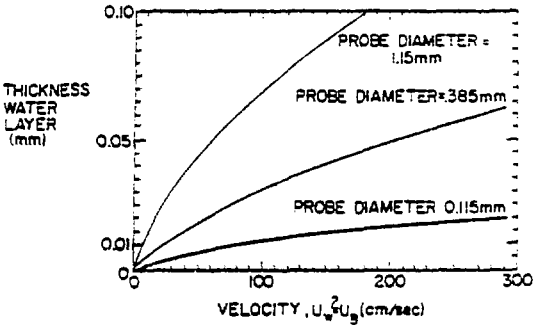

Figure 16 - Plot of water layer thickness vs. wire withdrawal velocity (Tallmadge and White[23]).
(BNL Neg. No. 3-1723-78)

the large angle tip (104°) was found to be strongly dependent on the water layer thickness left on the probe tip. In order to show this strong dependence of the probe output to the water layer left on the probe tip, we plot in Figure 15 the maximum angle β that can be sustained on a probe tip angle α before the coherent light rays ($\theta = 0$) are refracted out and the signal is zero. Within the α range of interest, $37 < \alpha < 65$, the maximum angle β increases, and the sensitivity of the probe to the water layer thickness decreases for the lower values of α.

For a possible explanation for the optical probe output behavior for various bubble velocities, it was proposed that a water film thickness left on the probe tip and increasing with the bubble velocity could explain the decrease in the signal intensity that was observed experimentally.

A literature search on wire withdrawal showed that the film thickness left along a small wire increases with withdrawal velocity (White and Tallmadge[21]. This theoretical

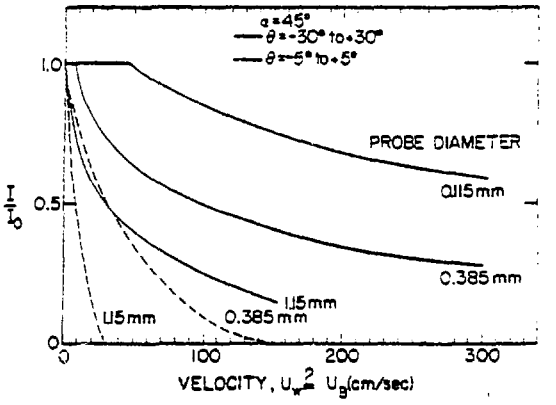

Figure 17 - Cross plot of normalized probe signal, I/I_o, vs. wire withdrawal velocity for three probe diameters and two values of the acceptance angle.
(BNL Neg. No. 31-1719-78)

prediction was also checked experimentally for various liquids. The dimensionless film thickness (Tallmadge and White[22] was related to a Capillary Number,

$$N_{ca} = \frac{\mu u_w}{\sigma} \tag{1}$$

and a Goucher Number,

$$N_{Go} = \frac{R}{a} \tag{2}$$

where μ and σ are the viscosity and surface tension of the liquid, u_w is the withdrawal velocity, R is the wire radius, and a is the capillary length defined as $(2\sigma/\rho g)^{1/2}$. In addition to this, White and Tallmadge[23] observed that experiments conducted with distilled water provided film thicknesses almost twice those predicted by the theory. This fact is still unexplained. In any event, the results may be used to obtain Figure 16 showing the increase in film thickness with increasing velocity.

The two parts of the theory explaining the probe behavior thus include:

a) Amplitude of signal vs. water film thickness;

b) Water film thickness vs. interface passage velocity.

A combination of the two will thus yield the predicted variation of signal amplitude with interfacial velocity as shown in Figure 17, in good qualitative agreement with the observed behavior. Differences may perhaps be explained by the presence of nonlinear films, slanted optical surfaces instead of surfaces colinear with the probe direction, etc.

r-f PROBE

The r-f probe presented in Figure 18 consisted of two 0.25 mm diameter insulated wires, with each wire encased in a 1 mm outside diameter stainless steel tube which were electrically connected to a common ground and acted as an electrical shield. The two shielding tubes themselves were encased in a larger stainless steel tube, which acts as a holder and provides rigidity. The sensitive part of the probe, the probe tip, was formed by extending the two insulated wires around 3 mm from the end of the shielding tubes. To prevent water from entering into the stainless steel tubes, each of the end connections were covered with a thin layer of epoxy including the tip of the two insulated wires which were also covered to insulate them from the surrounding media, water or air. When a d-c voltage is applied across one of the wires and the common ground, zero voltage is measured across the second wire and the ground. In operation of the probe, one of the wires is used as an emitter to which a sine wave is applied from a function generator. The second wire is used as a receiving antenna, and its output is fed directly to an oscilloscope or to a magnetic tape recorder after amplification. Similar r-f probes were previously described in the literature [24, 25] but a systematic study of the response characteristics was not undertaken. For a given amplitude and frequency of the input sine wave, the probe output signal has the same frequency as the input, but is out of phase. The amplitude of the output depends on whether the two insulated wires at the tip are in air or are completely immersed in water. The probe is sensitive to the dielectric constant of the media surrounding the tip.

The r-f probe was tested both in static air and water and with Taylor bubbles of known length and velocity in a simple test facility described briefly below.

First, the static response of the r-f probe in air and fully immersed in water was investigated in the test setup described above. When a sine wave with an amplitude of 22.7 v (peak-to-peak) was applied to the transmitting antenna (input), the amplitude of the received signal (output) varied with the signal frequency of the input (from 100 Hz to 10^7 Hz) both in air and in water. Figure 19 depicts the variation of the output, (A_{out}) divided by the input (A_{in}), both determined with an oscilloscope, as a function of the input sine wave frequency, when the probe tip is completely immersed in air or in water. Depending on the input frequency, the signal amplitude in water can be higher than the signal in air or vice-versa. The r-f probe seems to act as a band pass filter. For a 500 kHz, 22.7 peak-to-peak sine wave input, the output voltage of the r-f probe was also observed to be dependent on the static immersion depth of the insulated nonshielded portion of the probe tip into the water. The output increased linearly with the immersion depth, reached a maximum and then decreased and leveled off at the all water signal level. An additional fact observed was that the output versus input curve as presented in Figure 19 depends on the tube wall proximity.

Figure 20 presents the expanded output of the r-f probe during the passage of a bubble. The output decreases from its water level to the air level with the penetration into the bubble and stays almost constant during the passage of the bubble. When the water impinges on the probe tip again, the signal increases, passes through a maximum, decreases, and then levels off at the steady air level. A possible explanation for this maximum was proposed by Fortescue[26] as being due to the additional capacitance of the water surrounding the insulated unshielded

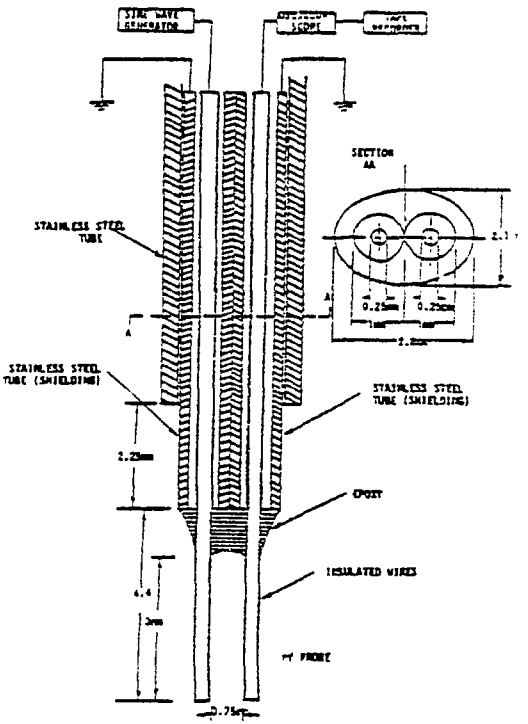

Figure 18 - Schematic Representation of the r-f Probe
(BNL Neg. No. 3-524-79)

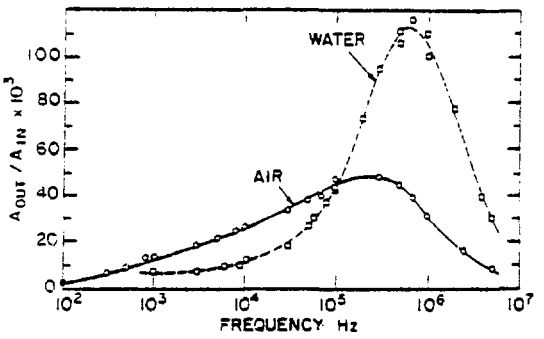

Figure 19 - Ratio of r-f Probe Output to Input Voltage Level as a Function of Input Sine Wave Frequency, for the Probe Tip in Air and in Water.
(BNL Neg. No. 3-529-79)

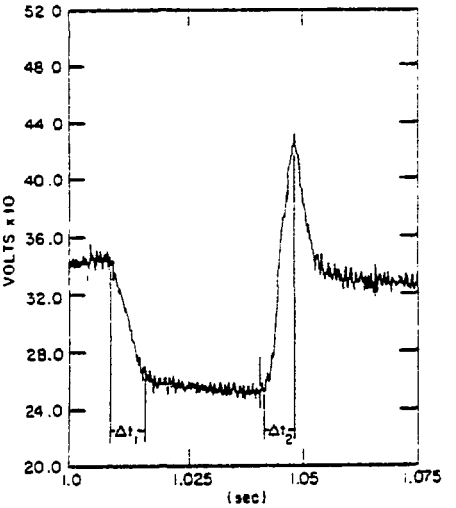

Figure 20 - Expanded Output of the r-f Probe During Passage of the Bubble.
(BNL Neg. No. 3-526-79)

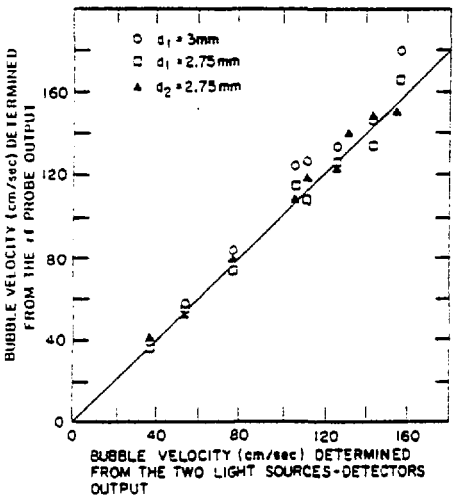

Figure 21 - Comparison of Bubble Velocity as Determined by Two Independent Methods, i.e., r-f Probe and Two Light Sources and Detectors.
(BNL Neg. No. 3-527-79)

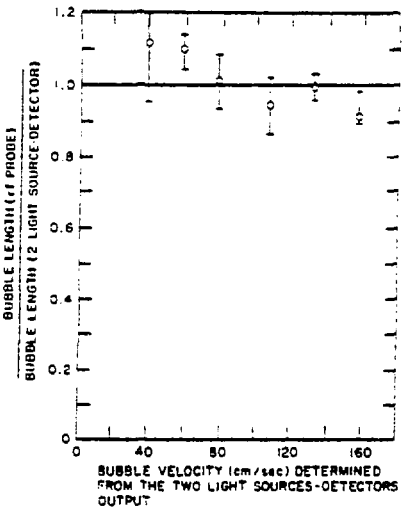

Figure 22 - Ratio of Bubble Length as Determined by the r-f Probe and the Two Light Source Detectors as a Function of Bubble Velocity.
(BNL Neg. No. 3-525-79)

wires. Grounding the water close to the tip by a separate copper wire eliminated this maximum of the probe signal.

In Figure 21, the bubble velocities determined by the r-f probe are compared with velocities determined from the output of the two light-source detectors. Two penetration time intervals were measured from the r-f probe output (Figure 20), Δt_1, and Δt_2. By considering a typical characteristic length of the sensitive part of the tip (3 mm and 2.75 mm), a bubble velocity was calculated by dividing the characteristic length by the time interval (Δt_1 of Δt_2). The actual dimension of the sensitive part of the tip is approximately 3 mm (see Figure 18). The bubble velocites determined by the two independent methods agree with each other within $\pm$ 10 percent. Thus with an r-f probe, the average bubble velocity can be determined from the passage time of either interface, air-water or water-air, along the insulated wires. This is true irrespective of the amplitude of the signal which may change with fluid state, purity, or test geometry.

The probe output levels for water and air did not change with the bubble velocity in the range considered (up to 160 cm/sec). Figure 22 depicts that the bubble sizes as determined by the two independent methods agree with each other with a maximum deviation of $\pm$ 10 percent. The bubble lengths recorded by the r-f probe are 10 percent higher at the low bubble velocities around 30 cm/sec. This fact may be due to surface tension effects during the penetration which become important at these low bubble velocities.

4. SUMMARY AND CONCLUSIONS

The current technology regarding void fluctuation dynamics was briefly summarized and new instrumentation developments undertaken at BNL were described. These instruments include a simplified, high intensity, low energy γ-densitometer utilizing simple solid state crystal detection techniques, an improved optical probe sensitive to both phase presence and liquid velocity, and a radio-frequency probe also capable of sensing phase presence and measuring interface velocity. The physics regarding liquid film interaction with small probes is discussed and it was shown how existing technology could be used to explain the optical probe behavior.

Specific conclusions include:

a. An optical probe with a new tip geometry capable of measuring local interface velocity, as well as void fraction was developed, constructed, and calibrated.

b. The new design, since it is encased in a stainless steel tube, is sufficiently strong to stand difficult environmental conditions.

c. A potential physical explanation for the probe behavior was identified.

d. A computer program to study the response characteristics of the various probe tip geometries was written and used in the analysis, confirming the experimental behavior.

e. An r-f probe of simple construction and geometry was described and shown capable also of measuring local void fraction and interface velocity.

5. REFERENCES

[1] Neal, L. S. and Bankoff, S. G., "A High Resolution Resistivity Probe for Determination of Local Void Properties in Gas-Liquid Flow," AIChE J., 9, 94-100, (1963).

[2] Lackme, C., "Statistical Analysis of the Local Structure of a Two-Phase Flow," CENG Notes TT-162 and TT-176, Grenoble, France, 1964.

[3] Akagawa, K., "Fluctuations in Void Ratio in Two-Phase Flow," Bull, J.S.M.E., 7, 122-128, (1964).

[4] Ishigai, S., Yamone, M., and Roko, K., "Measurement of the Component Flows in a Vertical Two-Phase Flow by Making Use of the Pressure Fluctuations," Bull. J.S.M.E., 8, 375-382, (1965).

[5] Jones, O. C., and Zuber, N., "The Interrelation Between Void Fraction Fluctuations and Flow Patterns in Two-Phase Flow," Int. J. Multiphase Flow, 2, 273-306, (1975).

[6] Jones, O. C., and Zuber, N., "Interfacial Passage Frequency for Two-Phase, Gas Liquid Flows in Narrow Rectangular Ducts," in Heat and Fluid Flow in Water Reactor Safety, pp. 5-10, IMechE, London, 1977.

[7] Lahey, R. T. - progress report on 60 Hz elim circuit for X-rays.

[8] LeLourneau, B. W., and Bergles, A. E., Ed., "Two-Phase Flow Instrumentation, ASME, (1969).

[9] Hewitt, G. F., and Lovegrove, P. C. "Experimental Methods in Two-Phase Flow Studies," EPRI Report NP-118, (1976).

[10] Delhaye, J. M., and Jones, O. C., "A Summary of Experimental Methods for Statistical and Transient Analysis of Two-Phase Gas Liquid Flow," Argonne Report ANL-76-75, (1976).

[11] Jones, O. C., and Delhaye, J. M., "Transient and Statistical Measurement Techniques for Two-Phase Flows: A Critical Review," Int. J. Multiphase Flow, 3, 89-116, (1976).

[12] Hsu, Y. Y., Ed., "Two Phase Flow Instrumentation Review Group Meeting," NUREG-0375, (1977).

[13] Jones, O. C., and Zuber, N., "Use of a Cylindrical Hot-Film Anemometer for Measurement of Two-Phase Void and Volume Flux Profiles in a Narrow Rectangular Duct," AIChE Sym. Ser., 74, 191-204, (1978).

[14] Serizawa, A., "Fluid-Dynamic Characteristics of Two-Phase Flow," PhD Thesis, Inst. of Atom. Ener., Kyoto Univ., Kyoto, Japan, (1974).

[15] Ohba, K., private communication, (1979).

[16] Danel, F., and Delhaye, J. M., "Sonde Optique pour Mesure du Taux de Presence Local en Ecoulement Diphasique," Mesures-Regulation-Automatisme, Aout-Septembre, 1971, pp. 99-101.

[17] Galaup, J. P., "Contribution a l'Etude des Methodes de Mesure en Ecoulement Diphasique," D.Sc. Thesis presented at the University Scientifique et Medicale de Grenoble et l'Institut National Polytechnique de Grenoble, 1975.

[18] Abuaf, N., Jones, O. C. Jr., and Zimmer, G. A., "Optical Probe for Local Void Fraction and Interface Velocity Measurements," Rev. Sci. Instruments, 1978, (in press).

[19] Abuaf, N., Jones, O. C., and Zimmer, G. A., "Response Characteristics of Optical Probes," ASME paper 78-WA/HT-3, presented at the ASME Winter Meeting, San Francisco, Ca., Dec. 10-15, (1978).

[20] Miller, N., and Mitchie, R. E., "Measurement of Local Voidage in Liquid/Gas Two-Phase Flow Systems," J. of British Nuclear Energy Society, 9, 2, 1970, pp. 94-100.

[21] White, D. A. and Tallmadge, J. A., "A Gravity Corrected Theory for Cylinder Withdrawal," AIChEJ, 13, 4, 1967, pp. 745-750.

[22] Tallmadge, J. A. and White, D. A., "Film Properties and Design Procedures in Cylinder Withdrawal," I&EC Process Design and Development, 7, 4, 1968, pp. 503-508.

[23] White, D. A. and Tallmadge, J. A., "A Theory of Withdrawal of Cylinders from Liquid Baths," AIChE J, 12, 2, 1966, pp. 233-339.

[24] Galaup, J. P., Thesis presented at the Universite Scientifique et Medicale de Grenoble et L'Institut National Polytechnique de Grenoble, 1975.

[25] Abuaf, N., Swoboda, A., Zimmer, G. A., Reactor Safety Research Programs, Quarterly Progress Report, BNL-NUREG-50747, p. 175, 1977.

[26] Fortescue, T., personal communication, 1978.

[27] Jones, O. C., "Inception and Development of Voids in Flashing Liquids," Paper presented at the Joint U.S.-Japan Seminar on Two-Phase Flow Dynamics, Osaka University, July 30-August 3, 1979.